by the enzyme and by the model catalyst.

The calculated KIE for $5 \rightarrow 6^{\ddagger}$ is dominated by the ZPE factor which is further analyzed in Table V. The major change in the ZPE factors for $5 \rightarrow 6^{\ddagger}$ vs. $3 \rightarrow 4^{\ddagger}$ is the smaller normal contribution from the CH rocking modes. The frequencies for these modes decrease as between reactants and transition state for both the catalyzed and uncatalyzed model reactions, but the size of the decrease is smaller in the case of catalysis with compression. Thus the overall ZPE factor for $5 \rightarrow 6^{\ddagger}$ is more inverse than that for $3 \rightarrow 4^{\ddagger}$.

The isotope effect $(V_{max}/K_m)^{CH_3}/(V_{max}/K_m)^{CD_3}$ determined by Schowen and co-workers[7] for the COMT-catalyzed reaction did not differ sensibly from the isotope effect $V_{max}^{CH_3}/V_{max}^{CD_3}$, implying that there was no α-D_3 isotope effect for binding of *S*-adenosylmethionine to the enzyme. As Table IV shows, however, there is a substantial calculated α-D_3 EIE of 0.812 for the equilibrium $3 \rightleftharpoons 5$ for binding of the reactant complex to the model catalyst. The error bounds for one standard deviation on the experimental $(V_{max}/K_m)^{CH_3}/(V_{max}/K_m)^{CD_3}$ value are actually sufficiently large as to permit the possibility of an inverse EIE for cofactor binding as large as the value calculated here for the model system; but since the nature of the binding interactions is certainly very different in the enzyme and in the model catalyst, it is perhaps not very remarkable if the EIEs for substrate binding are indeed significantly different.

Table IV also contains carbon-13 and carbon-14 KIEs calculated for the model methyl transfers. The value of $k(^{12}C)/k(^{13}C) = 1.072$ for the catalyzed process $5 \rightarrow 6^{\ddagger}$ is slightly larger than the value of 1.064 for the uncatalyzed reaction $1 + 2 \rightarrow 4^{\ddagger}$. The ZPE factor is dominating for both isotope effects. The experimental carbon-13 isotope effects are $V_{max}^{12}/V_{max}^{13} = 1.14 \pm 0.14$ for the COMT-catalyzed reaction[7] and $k(^{12}C)/k(^{13}C) = 1.08 \pm 0.02$ for methylation of methoxide by *S*-methyldibenzothiophenium tetrafluoroborate.[8] Thus the KIE for the enzyme-catalyzed reaction is probably larger than that for the uncatalyzed reaction, in accord with the results of the calculations for the model system. Once again it may be supposed that this similarity derives from the operation of a catalytic mechanism involving compression both for the COMT enzyme and for the model catalyst.

Conclusions

Despite its simplicity the model catalyst described in this work has successfully demonstrated the viability of catalysis of methyl transfer by a compression mechanism. It has been shown that the greater energetic penalty incurred by a compressed reactant state than by a compressed transition state allows the latter to be stabilized preferentially by a suitably designed catalyst, thereby causing a reduction in the activation energy. Preferential transition-state binding by the model catalyst does not occur in the absence of compression by repulsive interactions; on the contrary, the model reaction is actually inhibited by a "catalyst" which binds its substrates by attractive interactions only. Kinetic isotope effects calculated for catalyzed and uncatalyzed model reactions are in accord with trends in experimental isotope effects for enzymic and non-enzymic methyl transfers. Thus the theoretical model lends support to Schowen's hypothesis[5] concerning the possible role of compression in enzymic catalysis of methyl transfer. The importance of repulsive interactions between the catalyst and the substrate, at least for this class of group-transfer process, may have more general implications for design of synthetic catalysts. Simple juxtaposition of a catalytic site with a binding site affording attractive interactions only with a substrate may not necessarily permit differential binding (in the desired sense!) as between the reactant state and the transition state so as to provide catalysis.

Conformations of Cyclic Octapeptides. 1

Kenneth D. Kopple,* Kumarapuram N. Parameswaran, and James P. Yonan

Contribution from the Department of Chemistry, Illinois Institute of Technology, Chicago, Illinois 60616. *Received February 29, 1984*

Abstract: Four diastereoisomeric cylic octapeptides, *cyclo*(L- or D-Ala-Gly-L-Pro-L- or D-Phe)$_2$, were synthesized and characterized, and NMR data bearing on their conformations in dimethyl sulfoxide solution were obtained. The most stable backbones of these peptides have trans Gly–Pro peptide bonds and C_2 symmetry in the NMR average. The populations of the all-trans C_2 form range between 50 and 98%. Likely solution conformations of all-trans *cyclo*(D-Ala-Gly-L-Pro-D-Phe)$_2$ and *cyclo*-(L-Ala-Gly-L-Pro-L-Phe)$_2$ have turns at Pro-Phe. In both peptides two planes containing sequences of Gly, Pro, Phe, and Ala α-carbons are joined at roughly right angles along a line between the Ala α-carbons, and the Ala methyl groups are directed toward each other across the ring on the convex side of the fold. The proposed conformation for *cyclo*(L-Ala-Gly-L-Pro-L-Phe)$_2$ has two type I L-Pro-L-Phe β turns and is similar in important respects to the backbone of the crystalline cyclic octapeptide β-amanitin, except that β-amanitin contains both type I and type II turns. Data are presented for *cyclo*(L-Ala-Gly-L-Pro-D-Phe)$_2$, but a closely defined conformation is not obvious from them. Conformations of *cyclo*(D-Ala-Gly-L-Pro-L-Phe)$_2$ will be described in a subsequent paper.

Synthetic cyclic peptides of defined backbone conformation are potentially useful as analogues for determining biologically active conformations of naturally occurring peptides. Considerable progress has been made through NMR and X-ray investigations in determining the rules governing the relation between sequence and stable conformation for cyclic penta- and hexapeptides, particularly those containing the β turn as a well-defined conformational feature.[1-5] Because other cyclic peptide backbones may be of service as well, we now report studies to identify sequences producing stable cyclic octapeptide backbone conformations.

We desired to produce cyclic octapeptide backbones of C_2 symmetry determined by two β turns, using proline residues to locate the turns. Because the conformation of a peptide chain is determined to a first approximation by the sequence of glycines, prolines, and residues with a β-carbon, and by the α-carbon

(1) Gierasch, L. M.; Deber, C. M.; Madison, V.; Niu, C.-H.; Blout, E. R. *Biochemistry* **1981**, *20*, 4730–4738.
(2) Kopple, K. D. *Biopolymers* **1981**, *20*, 1913–1920.
(3) Bara, Y.; Friedrich, A.; Hehlein, W.; Kessler, H.; Kondor, P.; Molter, M.; Veith, H.-J. *Chem. Ber.* **1978**, *111*, 1045–1057.
(4) Pease, L. G.; Niu, C.-H.; Zimmermann, G. *J. Am. Chem. Soc.* **1979**, *101*, 184–191.
(5) Ovchinnikov, Yu. A.; Ivanov, V. T. "The Proteins", 3rd ed.; "The Cyclic Peptides: Structure, Conformation and Function", Neurath, H., Hill, R. L., Eds.; Academic Press: New York, 1980; Vol. 5, pp 491–538.

0002-7863/84/1506-7212$01.50/0

Table I. Blocked Intermediates in the Synthesis of *cyclo*(Ala-Gly-Pro-Phe)$_2$ Diastereomers

peptide	crystalization solvent	mp, °C	retention time, min	elemental anal.
Z-Ala-Gly-Pro-Phe-OMe	EtOAc	145–147	7.9[a]	$C_{28}H_{34}N_4O_7$: C, H, N
Z-D-Ala-Gly-Pro-Phe-OMe	EtOAc	155–157	7.9[a]	$C_{28}H_{34}N_4O_7$: C, H, N
Z-D-Ala-Gly-Pro-D-Phe-OMe	EtOAc	133–135	7.9[a]	$C_{28}H_{34}N_4O_7$: C, H, N
Z-Ala-Gly-Pro-D-Phe-OMe	EtOAc	165–167	12.2[b]	$C_{28}H_{34}N_4O_7$: C, H, N
Z-(Ala-Gly-Pro-Phe)$_2$-OMe	EtOH	199–202	13.4[a]	$C_{47}H_{58}N_8O_{11}\cdot H_2O$: C, H, N
Z-(D-Ala-Gly-Pro-Phe)$_2$-OMe	EtOAc	223–225	25.2[b]	$C_{47}H_{58}N_8O_{11}$: C, H, N
Z-(D-Ala-Gly-Pro-D-Phe)$_2$-OMe	EtOH	202–204	31[b]	$C_{47}H_{58}N_8O_{11}\cdot H_2O$: C, H, N

[a] 65% methanol–water, 1.0 mL/min, Whatman Partisil PXS 10–20 ODS-3 column. [b] 65% methanol–water, 1.0 mL/min, Whatman Partisil PXS 10/25 ODS-2 column.

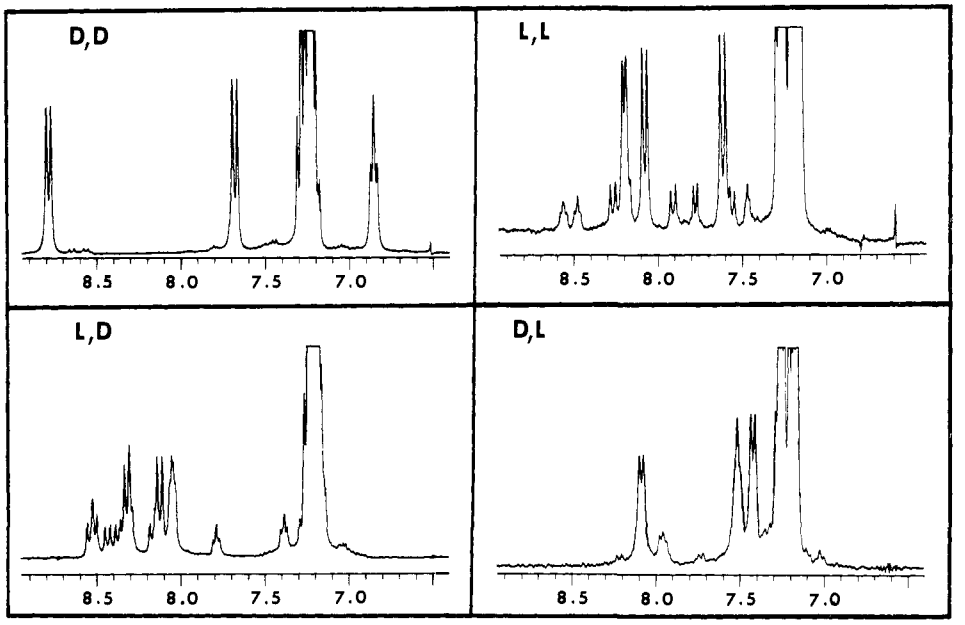

Figure 1. Peptide (NH) proton resonances of diastereomeric *cyclo*(Ala-Gly-L-Pro-Phe)$_2$ peptides in Me_2SO, 24 °C. The first letter gives the configuration at Ala and the second at Phe.

configurations, it is possible to search for backbone types by using residues easy to manipulate synthetically, in combinations with minimal spectral ambiguity. To minimize the fraction of cis X–Pro peptide bond conformation that would result from interference between the X side chain and Pro δ-methylene in the trans conformation,[6,7] we used the Gly-Pro sequence in this initial study. To explore the configuration variables, we examined analogues of *cyclo*(Y-Gly-L-Pro-Z)$_2$ containing combinations of D and L configurations at Y and Z. Ala and Phe were chosen for Y and Z, respectively. The resulting cyclic peptides are not water soluble, and they were examined chiefly in dimethyl sulfoxide (Me_2SO) solution.

The cyclic peptides were prepared by standard solution methods using active ester or mixed anhydride coupling to form tetrapeptides, which were then coupled to octapeptides via the azide method and cyclized by using the same method. Cyclization yields were in excess of 50% in all cases. All of the peptides were obtained in crystalline analytically pure form and shown to be cyclic octapeptides by fast atom bombardment (FAB) mass spectroscopy. The conformation analysis utilized the usual methods of proton and carbon NMR spectroscopy coupled with model building.

The most favored conformation of each of the four peptides was found to have trans Gly–Pro peptide bonds and exhibit C_2 symmetry in the NMR average. Solution conformations of the dominant all-trans forms of the D-Ala,D-Phe and L-Ala,L-Phe peptides are described in this paper. NMR data for the L-Ala,D-Phe peptide are also presented, but they do not closely define a conformation for the all-trans form. Crystal structures and solution conformation of the D-Ala,L-Phe isomer are described in a subsequent report.[8]

Experimental Procedures

Cyclic Octapeptides, *cyclo*(D- or L-Ala-Gly-L-Pro-D- or L-Phe)$_2$. The procedures customarily used in this laboratory for solution synthesis of cyclic peptides have been described recently.[9] In the present cases, benzyloxycarbonyl tetrapeptide methyl esters, Z-Ala-Gly-L-Pro-Phe-OMe, were prepared by stepwise condensation of benzyloxycarbonyl amino acid *N*-hydroxysuccinimide esters to C-terminal phenylalanine methyl ester of the appropriate configuration. Two tetrapeptide fragments were condensed to an octapeptide via the azide method, which was cyclized, again by the azide procedure. The cyclic octapeptides were isolated from the cyclization reaction mixture by removal of the solvent (dimethylformamide), trituration of the residue with water, precipitation from ethanol by water, and recrystallization from ethanol or ethanol–water.

Crystallized fully blocked tetra- and octapeptide intermediates were characterized by integration of their proton NMR spectra, elemental analyses, and retention time and purity in reversed-phase high-performance liquid chromatography (HPLC). The data are in Table I.

The diastereomeric cyclic octapeptides were characterized by analyses of 300-MHz proton and 75-MHz carbon NMR spectra, elemental analyses, HPLC, and fast atom bombardment (FAB) mass spectra in which the $(M + 1)^+$ ion at 745 was prominent for each peptide. Table II gives these data.

NMR Spectroscopy. Spectral data were obtained on a Nicolet NT 300 spectrometer, operating at 300 MHz for protons and 75 MHz for carbon. Peptide concentrations were 2–10 mM for proton NMR and 10–25 mM for carbon spectra. Nuclear Overhauser enhancements were

(6) Schimmel, P. R.; Flory, P. J. *J. Mol. Biol.* **1968**, *34*, 105–120.
(7) Kopple, K. D.; Sarkar, S. K.; Giacometti, G. *Biopolymers* **1981**, *20*, 1291–1303.
(8) Kartha, G.; Bhandary, K. K.; Kopple, K. D., manuscript in preparation. A preliminary report on one crystal of this peptide has appeared: "Abstracts", American Crystallographic Society Meeting, Denver, CO, Aug. 1–58 1983; Abstract PD14, p 32.
(9) Kopple, K. D.; Parameswaran, K. N. *Int. J. Pept. Protein Res.* **1983**, *21*, 269–280.

Table II. Diastereomers of *cyclic*(Ala-Gly-L-Pro-Phe)$_2$

configurations		cyclization		retention	% all-	
Ala	Phe	yield, %	mp, °C	time,[a] min	trans[b]	elemental anal.
L	L	43	309–312 dec	9.8	75	$C_{38}H_{48}N_8O_8$: C, H, N
L	D	44	315–318 dec	8.9	50	$C_{38}H_{48}N_8O_8 \cdot 2H_2O$: C, H, N
D	L	70	319–322 dec	7.6	90	$C_{38}H_{48}N_8O_8 \cdot 4H_2O$: C, H, N
D	D	54	318–321 dec	9.2	>98	$C_{38}H_{48}N_8O_8 \cdot 3H_2O$: C, H, N

[a] Whatman Partisil PXS 10/25 ODS2 column, 65% methanol–water, 1.0 mL/min. At 55% methanol the diastereomers eluted in the same order between 18 and 29 min. [b] Percentage of peptide present at 25 °C in Me_2SO in a form with C_2 average symmetry and trans Gly–Pro peptide bonds, determined from ^{13}C spectra and the N–H resonances of proton spectra.

Table III. NMR Data for *cyclo*(D-Ala-Gly-Pro-D-Phe)$_2$

	Me_2SO (23 °C)	MeOH (4 °C)	HFP (4 °C)
	N–H Protons		
Ala			
δ	7.68	7.84	7.51
$d\delta/dT$[a]	−0.0012	−0.0027	−0.0028
$k_{nitroxyl}$[b]	110	290	
J_{HNCH}	8.4	7.7	6.7
Gly			
δ	6.84	7.14	7.12
$d\delta/dT$[a]	+0.0003	−0.0001	<|.001|
$k_{nitroxyl}$[b]	100	150	
J_{HNCH}[c]	7.7, 6.7	5.1, 6.7[d]	7.2, 7.2
Phe			
δ	8.77	8.61	6.36
$d\delta/dT$[a]	−0.0043	−0.0068	−0.0027
$k_{nitroxyl}$[b]	450	2900	
J_{HNCH}	7.8	7.4	5.6
	α-Protons		
δ_{Ala}	4.18	4.28	4.36
δ_{Gly} (^2J)	4.05 (17.0)	4.16 (16.8)	4.26 (17.5)
	3.59	3.69	3.71
δ_{Pro}	4.19	4.23	4.58
δ_{Phe}	4.19	4.41	4.53
	β-Protons		
δ_{Phe} ($J_{\alpha,\beta}$)	3.20 (2.5)	3.30 (3.5)	3.24 (5.0)
	2.76 (12.0)	2.81 (11.2)	3.10 (8.3)
δ_{Pro}	1.92, 1.48	2.04, 1.64	2.15, 1.83
	Carbons		
$\delta_{Pro\ \beta}$	28.71	30.19	31.04
$\delta_{Pro\ \gamma}$	24.74	26.22	26.50

[a] Chemical shift temperature coefficient, ppm/deg. Negative coefficient correspond to shift upfield with increasing temperature. [b] Second-order rate constant, $M^{-1}\ s^{-1}$, for T_1 relaxation by 2,2,6,6-tetramethylpiperidinyl-1-oxy (Tempo). [c] Coupling to the higher field α-proton is given first. [d] Obtained by rapid-scan cross-correlation scanning between CH_3 and OH peaks. The 5.1-Hz value is ±0.5 Hz.

measured at 19°, just above the freezing point of the dimethyl sulfoxide solvent, to maximize the effects.

Results

The low-field regions of the proton resonance spectra of the four peptides in Me_2SO are compared in Figure 1. It can be seen that the D-Ala,D-Phe peptide exists almost entirely as a single component of average C_2 symmetry. The L-Ala,L-Phe compound is 75% in one C_2 form. Its principal minor form is unsymmetrical. In the D-Ala,L-Phe peptide the chief minor component (10%) appears also to be unsymmetrical, although not all of its N–H resonances are visible. The L-Ala,D-Phe peptide is only 50% in its major C_2 form. The principal minor form of this peptide again appears to be the unsymmetrical one, but indications of a third form are visible. In all cases, the ^{13}C chemical shift differences between proline β- and γ-carbons show the major C_2-symmetric components to have trans Gly–Pro peptide bonds, and the unsymmetrical minor components to have one cis and one trans Gly–Pro bond.[10] The individual peptides, except for the D-Ala,L-Phe isomer, are described in more detail below.

Table IV. Conformational Constants Derived from NMR Data for *cyclo*(D-Ala-Gly-Pro-D-phe)$_2$ in Me_2SO

observation (see tables III and V)	conformational constraint	ref[a]
$^3J_{HNCH}$	$\phi_{D\text{-}Ala}$ = +100 ± 5° or +140 ± 5°	12, 13[b]
NOE Gly H^N – Ala H^N	$\psi_{D\text{-}Ala}$ nearer 0° than 180°	*c*
nitroxyl relaxation	Ala N–H sequestered	14, 15
$^3J_{HNCH}$	ϕ_{Gly} = ±80 ± 5°	12, 13[b]
$^2J_{HCH}$ (Gly)	ψ_{Gly} = ±155 ± 10° if ϕ_{Gly} = ±80°	16
nitroxyl relaxation	Gly N–H sequestered	14, 15
$^3J_{HNCH}$	$\phi_{D\text{-}Phe}$ = +95 ± 5° or +145 ± 5°	12, 13[b]
$\Delta\delta_{\beta\gamma}$ (Pro C)	ψ_{Pro} = +150° or −30°	10
NOE Phe H^N – Pro H^α	ψ_{Pro} = 150° rather than −30°	*c*
$^3J_{HCCH}$ (Phe)	χ^1_{Phe} = predominantly +60° or 180°	17
$\delta_{Pro\ H^\beta}$	χ^1_{Phe} = +60° rather than 180°	*d*

[a] References are given to papers describing the relationship used to obtain the conformational constraint from the NMR observation. [b] The J_{HNCH} correlations cited are those we consider to have the best experimental bases for the present purpose. Within the ranges given they give similar dihedral angles, but the true uncertainties are undoubtedly larger. [c] NOE data are not used quantitatively, but to distinguish between pairs of possibilities with significantly different interproton distances. [d] One Pro H^β about 0.5 ppm above the usual chemical shift, ascribed to the Phe ring current effect.

***cyclo*(D-Ala-Gly-L-Pro-D-Phe)$_2$.** *cyclo*(D-Ala-Gly-L-Pro-D-Phe)$_2$ could be examined in dimethyl sulfoxide, methanol, and hexafluoro-2-propanol. In all three solvents the dominant form has trans Gly-Pro peptide bonds and C_2 symmetry in the NMR average. Components with cis Gly–Pro bonds are present to the extent of no more than 2% in Me_2SO and are undetected (<1%) in methanol or hexafluoro-2-propanol. Key NMR data are given in Table III. Certain features of the observations suggest that there is a well-defined backbone conformation with sequestered Gly and Ala H^N. First, The N–H proton resonances span large ranges, 1.9 ppm in Me_2SO and 1.5 ppm in methanol. In a solvated random conformational distribution, Phe, Ala, and Gly H^N resonances would all be expected to be grouped within a few tenths of a ppm.[11] Second, the Phe H^N is four times as sensitive to relaxation by nitroxyl as are the H^N of Gly and Ala in Me_2SO, and at least ten times as sensitive in methanol: this is the largest differentiation we have so far observed. Third, the chemical shifts of the Gly and Ala H^N are constant within 0.3 ppm in the three solvents, while the Phe H^N moves upfield 2.3–2.4 ppm in hexafluoro-2-propanol. Finally, in all three solvents the geminal H^α of the Gly residues differ in chemical shift by about 0.5 ppm, more than the usual difference when there is no adjacent aromatic residue. Therefore it seems reasonable to construct a model of the backbone conformation by using constraints derived from the NMR observations, and it is likely that this conformation is retained in all three solvents. Table IV lists the constraints and the observations from which they are derived.

(10) Siemion, I. Z.; Wieland, T.; Pook, K.-H. *Angew. Chem., Int. Ed. Engl.* **1975**, *14*, 702–703.

(11) Bundi et al. (Bundi, A.; Wuthrich, K. *Biopolymers* **1979**, *18*, 285–297) give data for aqueous solutions of tetrapeptide models; experience indicates that this is true for dipeptide models in Me_2SO also.

Table V. Intramolecular Proton–Proton Nuclear Overhauser Enhancements for *cyclo*(D-Ala-Gly-L-Pro-D-Phe)$_2$ in Me_2SO[a]

proton irradiated	proton observed: Ala H^N	Gly H^N	Phe H^N	Ala, Pro, Phe H^α	Gly H^α (high)	Gly H^α (low)
Ala H^N		7	3	5[b]		
Gly H^N	6				1	3
Phe H^N	4	1		15[b,c]		
Ala, Pro, Phe H^α	3	1	6			
Gly H^α (high)		3				20
Gly H^α (low)		2			18	

[a] Enhancements are in percent and are negative. The values were determined from the relative areas of a difference spectrum and a spectrum measured with irradiation off any resonance. [b] These values are given on the assumption that only one of the three proton resonances under this peak is affected. [c] See Figure 2.

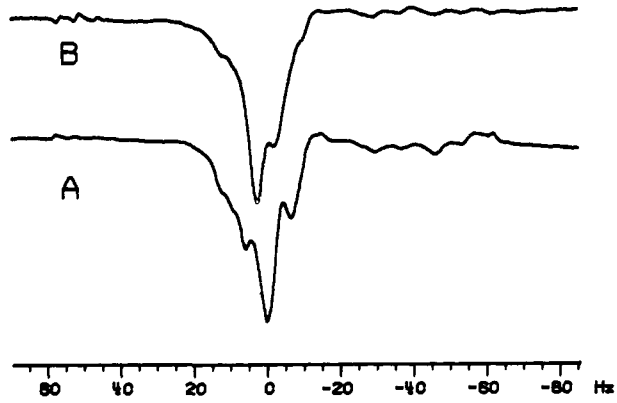

Figure 2. NOE difference spectra of overlapping Phe, Pro, and Ala α-proton resonances showing NOE resulting from irradiation of Phe H^N of *cyclo*(D-Ala-Gly-Pro-D-Phe)$_2$ in Me_2SO: A, irradiation of overlapping Pro H^γ and lower field H^β resonances during acquisition (A is identical with the pattern obtained when irradiation during acquisition is not on any resonance); B, irradiation of the more strongly coupled Phe H^β during acquisition, showing loss of coupling.

Included in Table IV are conclusions from nuclear Overhauser enhancements. NOE's were observed in Me_2SO solution, although not in the less viscous methanol or HFP, presumably for reasons of rotational reorientation time. The (negative) enhancements observed in Me_2SO are given in Table V. The largest conformationally important effect among the backbone H^N and H^α is an effect on the pattern of overlapping Phe, Ala, and Pro α-proton resonances upon irradiation of the Phe H^N. If only one of the three α-protons is actually affected, this enhancement is −15%, comparable in magnitude to the interaction between the geminal Gly α-protons. By making measurements with decoupling at the β-protons of Phe and Pro (see Figure 2), it was established that the observed NOE is the result of dipolar coupling between Pro H^α and Phe H^N. This result indicates a value for μ_{Pro} near 120°.

A −(6–7)% effect on the Gly H^N was observed on irradiation of Ala H^N and vice versa, which suggests that the conformation of the D-Ala residue is one that brings these two N–H protons into proximity. Their closest possible approach would be at $\phi_{Ala} = 180°$, $\psi_{Ala} = 0°$.

Four models consistent with the constraints of Table IV can be constructed. They are described by the sets of approximate dihedral angles (deg) below:

	Ala		Gly		Pro		Phe	
	ϕ	ψ	ϕ	ψ	ϕ	ψ	ϕ	ψ
A	140	50	−80	180	−60	150	95	−60
B	100	40	−80	180	−60	150	95	−20
				and				
C	140	40	80	180	−60	150	145	−30
D	100	40	80	180	−60	150	145	20

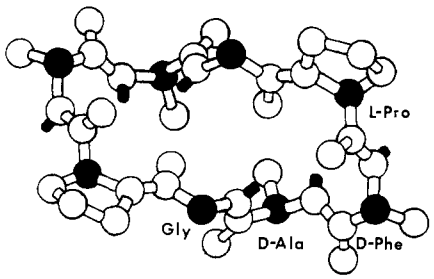

Figure 3. Drawing of proposed conformation B of *cyclo*(D-Ala-Gly-L-Pro-D-Phe)$_2$. The view is from the concave side of the fold.

Conformations A and B are twisted structures that differ by rotation of the plane of the CONH group between D-Phe and D-Ala. In A the most likely intramolecular hydrogen bond is a C_7 ring at Phe. In B there can be 10-membered-ring hydrogen bonds, Phe N–H to Gly C=O and/or Gly N–H to Pro C=O. The L-Pro-D-Phe sequence forms an approximate type II β-turn, and is followed by an approximate type III′ D-Phe-D-Ala turn. In both A and B the Phe N–H is much more exposed to solvent than is either the Gly or Ala N–H, which is in accord with the nitroxyl relaxation rates.

Backbones A and B are formed by two planes containing the α-carbons of Ala-Gly-Pro-Phe-Ala sequences joined at roughly right angles along a line between the Ala α-carbons. The Ala methyl groups are directed toward each other on the convex side of the fold. A drawing of conformation B, in which the two halves are more nearly planar, is given in Figure 3.

A clear distinction between A and B is probably not possible with the data available. Model A (Phe C_7) is suggested by the Overhauser effects between the α-proton group and the Ala H^N, assuming these effects involve Phe H^α. On the other hand, the interaction between Phe H^N and Ala H^N supports B, which has these two protons in greater proximity than does A. A quantitative analysis with the data of Table V would be out of place, considering that the dihedral angles estimated from the NMR data are only approximations, and that small variations in these can result in important variations in internuclear distances.

Conformations C and D are open structures with no juxtaposition of C=O and N–H groups. Although C and D are consistent with much of the NMR data, models of them give no reason to expect the large observed difference in solvent exposure between the Phe and Gly H^N. C and D are therefore unlikely models of the solution conformation.

The structure of a crystal of *cyclo*(D-Ala-Gly-L-Pro-D-Phe)$_2$ has recently been solved. The backbone conformation found in the crystal is very similar to conformation B.[18]

***cyclo*(L-Ala-Gly-L-Pro-L-Phe)$_2$.** NMR data for *cyclo*(L-Ala-Gly-L-Pro-L-Phe)$_2$ in Me_2SO are given in Table VI. No nuclear Overhauser effects above the 2% level were found to relate the backbone protons in Me_2SO. The peptide is extremely insoluble in methanol. Although it is soluble in hexafluoro-2-propanol, we were unable to analyze the low-field H^N region in that solvent.

There are indications that *cyclo*(L-Ala-Gly-L-Pro-L-Phe)$_2$ in Me_2SO has a single all-trans conformation with little averaging, particularly in regard to the Gly residue. The two Gly HNCH coupling constants are 7.8 Hz and less than 2 Hz; a 2-Hz observed coupling is only possible if the corresponding dihedral angle re-

(12) Ramachandran, G. N.; Chandrasekaran, R.; Kopple, K. D. *Biopolymers* **1971**, *10*, 2113–2131.
(13) DeMarco, A.; Llinas, M.; Wuthrich, K. *Biopolymers* **1978**, *17*, 637–650.
(14) Kopple, K. D. *Int. J. Pept. Protein Res.* **1983**, *21*, 43–48.
(15) Niccolai, N.; Valensin, G.; Rossi, C.; Gibbons, W. A. *J. Am. Chem. Soc.* **1982**, *104*, 1534–1537.
(16) Barfield, M.; Hruby, V. J.; Meraldi, J.-P. *J. Am. Chem. Soc.* **1976**, *98*, 1308–1314.
(17) Kopple, K. D.; Wiley, G. R.; Tauke, R. *Biopolymers* **1973**, *12*, 627–636.
(18) Kartha, G.; Bhandary, K. K., private communication. Reported at the International Union of Crystallography meeting, Hamburg, July 1984.

Table VI. NMR Data for *cyclo*(L-Ala-Gly-L-Pro-L-Phe)$_2$ and *cyclo*(L-Ala-Gly-L-Pro-D-Phe)$_2$ in Me_2SO, 23 °C

	L-Ala,L-Phe	L-Ala,D-Phe
	N-H Protons	
Ala		
δ	7.62	8.08
$d\delta/dT$[a]	−0.001	−0.0054
$k_{nitroxyl}$[b]	120	210
J_{HNCH}	8.8	9.0
Gly		
δ	8.20	8.02
$d\delta/dT$[a]	−0.003	−0.0042
$k_{nitroxyl}$[b]	140	190
J_{HNCH}[c]	<2, 7.8	3–4, ca. 7
Phe		
δ	8.09	8.33
$d\delta/dT$[a]	−0.0026	−0.0014
$k_{nitroxyl}$[b]	250	320
J_{HNCH}	8.1	8.7
	α-Protons	
δ_{Ala}	4.45	4.45
δ_{Gly} (^2J)	4.51 (17.8)	4.10 (18)
	3.87	3.76
δ_{Pro}	3.98	4.25
δ_{Phe}	4.27	4.58
	β-Protons	
δ_{Phe} ($J_{\alpha\beta}$)	3.25 (<5)	
	2.76 (12.2)	
δ_{Pro}	1.90, 1.40	
	Carbons	
$\delta_{Pro\ \beta}$	28.52	28.85
$\delta_{Pro\ \gamma}$	24.13	24.39

[a] Chemical shift temperature coefficient, ppm/deg. Negative coefficients correspond to shift upfield with increasing temperature. [b] Second-order rate constant, $M^{-1}\ s^{-1}$, for T_1 relaxation by 2,2,6,6-tetramethylpiperidinyl-1-oxy (Tempo). [c] Coupling to the higher field α-proton is given first. The 2-Hz value was obtained from the difference in line widths when H^N is irradiated and not.

Table VII. Conformational Constraints from NMR Data for *cyclo*(L-Ala-Gly-L-Pro-L-Phe)$_2$ in Me_2SO

observation (see Table VI)	conformational constraint	ref[a]
$^3J_{HNCH}$	$\phi_{Ala} = -120 \pm 15°$	12, 13[b]
	$\phi_{Gly} = \pm(155 \pm 10°)$	
	$\phi_{Phe} = -140 \pm 5°$ or $-100 \pm 5°$	
$^2J_{HCH}$ (Gly)	ψ_{Gly} near 180°	16
$\Delta\delta_{\beta\gamma}$ (Pro C)	$\psi_{Pro} = 160°$ or $-40°$	10
$^3J_{HCCH}$ (Phe)	χ^1 = predominantly −60° or 180°	17
$\delta_{Pro\ H^\beta}$	$\chi^1_{(Phe)} = -60°$ rather than 180°	c

[a] References are given to papers describing the relationship used to obtain the conformational constraint from the NMR observation. [b] The J_{HNCH} correlations cited are those we consider to have the best experimental bases for the present purpose. Within the ranges given they give similar dihedral angles, but the true uncertainties are undoubtedly larger. [c] One Pro H^β about 0.5 ppm above the usual chemical shift, ascribed to the Phe ring current effect.

mains close to 90° most of the time. The nonequivalence of the Gly H^α pair is .64 ppm, with one of the protons unusually far downfield at 4.51 ppm. Also supporting conformational restriction is the distinctly above average coupling constant for the Ala NHCH unit (8.8 Hz). The constraints indicated by the NMR data on the assumption of a single conformation for the all-trans form are given in Table VII. In addition, the absence of observable nuclear Overhauser interaction between the Pro α and Phe H^N protons, under conditions in which the D-Ala,D-Phe isomer exhibits a definitive effect, restricts ψ_{Pro} to the −40° value. The nitrosyl relaxation rate data show that the Gly and Ala H^N are certainly sequestered and that approach by nitroxyl to Phe H^N is probably hindered to some extent. None of the peptide bond protons is fully solvent exposed by the temperature coefficient criterion. Models can be constructed consistent with these constraints by using the following sets of approximate dihedral angles (deg):

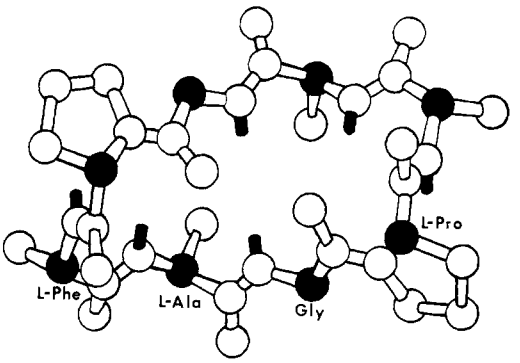

Figure 4. Drawing of proposed conformation A of *cyclo*(L-Ala-Gly-L-Pro-L-Phe)$_2$. The view is from the concave side of the fold.

	Ala		Gly		Pro		Phe	
	ϕ	ψ	ϕ	ψ	ϕ	ψ	ϕ	ψ
A	−120	−60	−150	180	−60	−40	−100	0
B	−120	−60	−150	180	−60	−40	−140	30
				and				
C	−120	0	150	180	−60	−40	−100	0
D	−120	0	150	180	−60	−40	−140	30

These four possibilities are all twisted rings of substantially the same shape, with a type I β turn at Pro-Phe. The β structures formed by the Gly-Pro-Phe sequences are planes meeting along a line joining the Ala α-carbons, and the Ala methyl groups are directed toward each other on the convex side of the dihedral. The ala N-H bonds are directed into the ring, and the Phe N-H bonds are directed roughly perpendicularly to the β-turn planes, partially shielded by the ring of Pro and the side chain of Phe. In A and B the Gly N-H are directed into the ring; in and D the Gly N-H are directed into the angle between the two β-turn planes. Space-filling models suggest that there is substantially greater solvent exposure of the Gly H^N in the latter case. Since the Gly H^N show the same sensitivity to nitroxyl relaxation as the definitely buried Ala H^N, conformations A or B seem more likely. Conformation A is drawn in Figure 4.

Conformation A of *cyclo*(L-Ala-Gly-L-Pro-L-Phe)$_2$ is very much like a doubling of that half of the crystal conformation of the cyclic octapeptide β-amanitin[19] that contains a type I Hyp-diOH-Ile turn:

L-Cys		L-Asp		L-Hyp		L-diOH-Ile		L-Trp	
ϕ	ψ	ϕ	ψ	ϕ	ψ	ϕ	ψ	ϕ	ψ
−121	−85	−172	179	−60	−37	−79	−23	−109	−40

Although β-amanitin, which has the sequence *cyclo*(Trp-Gly-Ile-Gly-Cys-Asp-Hyp-diOH-Ile), has a type II β turn at Ile-Gly, the folding of the peptide ring is similar to that of conformations A or B just described, i.e., two β-structure planes meeting along the line joining the Trp and Cys α-carbons. In β-amanitin the transannularly proximate side chains of Trp and Cys, corresponding to the Ala CH_3's in the present peptides, are joined by oxidative coupling at the 2-position of the indole ring.

***cyclo*(L-Ala-Gly-L-Pro-D-Phe)$_2$.** Although there is interference by the resonances of the minor components, most of the backbone resonance data for the all-trans form of *cyclo*(L-Ala-Gly-L-Pro-D-Phe)$_2$ were obtained. They are given in Table VI. Clearly observed nuclear Overhauser enhancements found in Me_2SO are −6% on the Pro H^α resonance when Phe H^N is irradiated and −5% on the Phe H^α when Ala H^N is irradiated. The only evidences of a narrowly defined conformation are the high H-N-C-H couplings for Phe and Ala. On the other hand, observations suggesting averaging are that the chemical shift range of the N-H resonances is only 0.3 ppm and that the Gly H^α resonances differ by only 0.34 ppm. Also, the nitroxyl and temperature coefficient

(19) Kostansek, E. C.; Lipscomb, W. N.; Yocum, R. R.; Thiessen, W. E. *Biochemistry* **1978**, *17*, 3790–3795.

Table VIII. Conformational Constraints from NMR Data for *cyclo*(L-Ala-Gly-L-Pro-D-Phe)$_2$ in Me_2SO

observation (see Table VI)	conformational constraint	ref[a]
$^3J_{HNCH}$	$\phi_{Ala} = -120 \pm 15°$	12, 13[b]
	ϕ_{Gly} = ca. $\pm 90°$	
	$\phi_{Phe} = 120 \pm 15°$	
$^2J_{HCH}$ (Gly)	ψ_{Gly} near 180°	16
$\Delta\delta_{\beta\gamma}$ (Pro C)	ψ_{Pro} = 165° or −45°	10
NOE Phe H^N - Pro H^α	ψ_{Pro} = 165° rather than −45°	*c*

[a] References are given to papers describing the relationship used to obtain the conformational constraint from the NMR observation. [b] The J_{HNCH} correlations cited are those we consider to have the best experimental bases for the present purpose. Within the ranges given they give similar dihedral angles, but the true uncertainties are undoubtedly larger. [c] NOE data are not used quantitatively, but to distinguish between pairs of possibilities with significantly different interproton distances.

data do not suggest an obvious mutually consistent interpretation. If a single conformation is important, the NMR constraints on it would be those given in Table VIII. Within those constraints models with the approximate dihedral angles below can be constructed, but they are not suggested with confidence. They differ primarily in the orientation of the Ala–Gly peptide bond.

	Ala		Gly		Pro		D-Phe	
	ϕ	ψ	ϕ	ψ	ϕ	ψ	ϕ	ψ
A	−120	0	90	180	−60	165	120	−40
B	−120	−160	−90	180	−60	165	120	−60

Conclusions

Cyclic octapeptides cannot form the complete cyclic β structures that can be approximated by cyclic hexapeptides (two joined β turns) or cyclic decapeptides like gramicidin S (two β turns linked by two extended residues). However, cyclic octapeptides that will adopt C_2 symmetric average conformations with two β turns can apparently be designed. Of the four diastereomers prepared in this work, the two that have the most closely defined conformations in solution are *cyclo*(D-Ala-Gly-L-Pro-D-Phe)$_2$ and *cyclo*(L-Ala-Gly-L-Pro-L-Phe)$_2$. Their conformations are similar: planes formed by the α-carbons of the Ala-Gly-Pro-Phe-Ala sequences, which include Pro-Phe turns, meet along a line joining the Ala α-carbons. The β turns are type I for L-Pro-L-Phe and type II for L-Pro-D-Phe)$_2$, as expected. The fold at the Ala C^α is such as to place the Ala side chains on its convex side, so that very roughly speaking the backbone of the ring containing L-Ala is a reflection of the ring containing D-Ala. To generalize from this result, it may be expected that cyclic octapeptides in which β turns are caused to exist at residues 2,3 and 6,7 will tend to adopt such a dihedral structure folded along the 4–8 line if 4 and 8 are of the same configuration. It would be of interest to test whether stable conformations occur if 4 and 8 are of opposite configurations. Further discussion of this kind of backbone will be offered in a subsequent paper on *cyclo*(D-Ala-Gly-Pro-L-Phe)$_2$.

Acknowledgment. This research was supported by grants from the National Institute of General Medical Sciences, GM 26071 and GM 26071-02S1 (300-MHz NMR instrument). The FAB mass spectra were obtained by Dr. Kenneth B. Tomer of the Midwest Center for Mass Spectrometry, University of Nebraska, Lincoln, a NSF Regional Instrumentation Facility.

Registry No. *cyclo*(L-Ala-Gly-L-Pro-L-Phe), 91383-23-2; *cyclo*(L-Ala-Gly-L-Pro-D-Phe), 91383-24-3; *cyclo*(D-Ala-Gly-L-Pro-L-Phe), 91383-22-1; *cyclo*(D-Ala-Gly-L-Pro-D-Phe), 91302-75-9; Z-Ala-Gly-Pro-Phe-OMe, 91302-78-2; Z-D-Ala-Gly-Pro-Phe-OMe, 91302-77-1; Z-D-Ala-Gly-Pro-D-Phe-OMe, 91302-76-0; Z-Ala-Gly-Pro-D-Phe-OMe, 91302-79-3; Z-(Ala-Gly-Pro-Phe)$_2$-OMe, 91949-02-9; Z-(D-Ala-Gly-Pro-Phe)$_2$-OMe, 91949-03-0; Z-(D-Ala-Gly-Pro-D-Phe)$_2$-OMe, 91949-04-1.

Steric Course of the Allylic Rearrangement Catalyzed by β-Hydroxydecanoylthioester Dehydrase. Mechanistic Implications

John M. Schwab* and John B. Klassen

Contribution from the Department of Chemistry, The Catholic University of America, Washington, DC 20064. *Received March 19, 1984*

Abstract: β-Hydroxydecanoylthioester dehydrase, which is the pivotal enzyme in the biosynthesis of unsaturated fatty acids in anaerobic metabolism, catalyzes the equilibration of thio esters of (*R*)-3-hydroxydecanoic acid, (*E*)-2-decenoic acid, and (*Z*)-3-decenoic acid. On the basis of evidence available to date, both two-base and one-base mechanisms of action can be envisioned for dehydrase. In an effort to distinguish between these mechanisms, the stereochemical course of the dehydrase-catalyzed allylic rearrangement has been determined. *N*-Acetylcysteamine (NAC) thio esters of (*R*)- and (*S*)-(*E*)-[4,5,5-$^2H_3$]decanoic acid were synthesized and incubated with dehydrase. The product (*Z*)-3-decenoyl-NAC was derivatized, and ^2H NMR analysis showed that the *pro*-4*R* hydrogen had been removed. (*E*)-2-[2-^2H]Decenoyl-NAC and unlabeled (*E*)-2-decenoyl-NAC were incubated with dehydrase in ^1H_2O and ^2H_2O, respectively. Analysis of a derivative of the resulting labeled (*Z*)-3-decenoyl-NAC showed that protonation had occurred on the *si* face at substrate C-2. The overall steric course of the reaction is therefore suprafacial. The significance of this result is discussed in terms of the mechanisms of the "normal" dehydrase-catalyzed reactions as well as the "suicide" inactivation of the enzyme.

While the overall scheme for biosynthesis of saturated fatty acids[1] is essentially invariant throughout nature, there are fundamental differences in the ways in which unsaturated fatty acids are assembled[2] in aerobic and anaerobic metabolism. In aerobes, a double bond is introduced at an isolated position in a preformed saturated fatty acid (often 16, 18, or 20 carbon atoms in length). The enzyme responsible is a membrane-bound fatty acid desaturase system that requires NADPH and molecular oxygen. Obviously, anaerobes cannot utilize oxygen, and so as an alternative, they synthesize unsaturated fatty acids de novo. The pivotal step in this pathway is catalyzed by β-hydroxydecanoylthioester dehydrase[3] ("dehydrase"), a bifunctional enzyme that mediates

(1) Zubay, G. "Biochemistry"; Addison-Wesley: Reading, MA, 1983; pp 487–495.
(2) Bloch, K. *Acc. Chem. Res.* **1969**, *2*, 193–202.

0002-7863/84/1506-7217$01.50/0